



This article was originally published in a journal published by Elsevier, and the attached copy is provided by Elsevier for the author's benefit and for the benefit of the author's institution, for non-commercial research and educational use including without limitation use in instruction at your institution, sending it to specific colleagues that you know, and providing a copy to your institution's administrator.

All other uses, reproduction and distribution, including without limitation commercial reprints, selling or licensing copies or access, or posting on open internet sites, your personal or institution's website or repository, are prohibited. For exceptions, permission may be sought for such use through Elsevier's permissions site at:

<http://www.elsevier.com/locate/permissionusematerial>

## Auditory evoked responses in the rat: Transverse mastoid needle electrodes register before cochlear nucleus and do not reflect later inferior colliculus activity

Junli Ping<sup>a</sup>, Nanxin Li<sup>a</sup>, Yi Du<sup>a</sup>, Xihong Wu<sup>a,b</sup>, Liang Li<sup>a,b,c</sup>, Gary Galbraith<sup>d,\*</sup>

<sup>a</sup> Department of Psychology, Peking University, Beijing 100871, People's Republic of China

<sup>b</sup> National Key Laboratory on Machine Perception, Speech and Hearing Research Center, Peking University, Beijing 100871, People's Republic of China

<sup>c</sup> Department of Psychology, Centre for Research on Biological Communication Systems, University of Toronto at Mississauga, Mississauga, Ontario, Canada L5L 1C6

<sup>d</sup> Department of Psychiatry and Biobehavioral Sciences, David Geffen School of Medicine, University of California at Los Angeles, c/o MRRC-UCLA Research Group, Lanterman Developmental Center, P.O. Box 100-R, Pomona, CA 91769, USA

Received 21 May 2006; received in revised form 13 September 2006; accepted 2 October 2006

### Abstract

A previously described technique putatively differentiates short-latency auditory evoked potentials in peripheral and central neural pathways of the mouse and rat [Galbraith G, Waschek J, Armstrong B, Edmond J, Lopez I, Liu W, et al. Murine auditory brainstem evoked response: putative two-channel differentiation of peripheral and central neural pathways. *J Neurosci Methods* 2006;153:214–20]. This technique involves recording from orthogonally oriented subdermal needle electrode pairs, using fast sample rates (100 k/s) to accurately measure differences in neural timing and waveform morphology. Electrodes oriented in a transverse plane (mastoid-to-mastoid) register an initial positive-going peak earlier than peaks recorded from electrodes oriented along the scalp midline (anterior and posterior to the interang

recordings may confound inherently distinct signals propagating over peripheral and central auditory pathways differing in location and orientation.

Galbraith et al. (2006) have shown in mice and rats that horizontally oriented subdermal electrodes (i.e., mastoid-to-mastoid) record short-latency (<1 ms) responses with a putative origin in the auditory nerve; while orthogonally oriented midline electrodes (anterior and posterior to the interaural line) register activities at longer, and thus more central, latencies. In the present study, we simultaneously record from transverse subdermal mastoid (M) needle electrodes and electrodes acutely implanted in dorsal cochlear nucleus (CN) and inferior colliculus (IC) of the rat. The results show that the initial M response occurs prior to a CN response, and is non-existent during later IC response components. These results indicate that the M response is a relatively isolated measure of neural activity generated immediately prior to reaching the central nervous system (CNS), suggesting an obligatory site of origin in the auditory nerve (AN).

The ability to more effectively isolate and unambiguously measure different short-latency evoked potential components using non-invasive recording techniques will lead to improved longitudinal assessments of the same animals throughout growth and neural development.

## 2. Materials and methods

### 2.1. Animal preparation

Fifteen male Sprague–Dawley rats (age 10–12 weeks, weight 280–320 g) were obtained from Beijing Vital River Experimental Animals Technology Ltd. (Beijing, China). They were anesthetized with chloral hydrate (400 mg/kg, i.p.) and placed in a Kopf small animal stereotaxic instrument. The scalp was incised, the skull exposed, and 0.75 mm diameter holes drilled at appropriate anterior–lateral stereotaxic coordinates. Metal electrodes insulated except at the 0.25 mm diameter tip were then lowered to the target depth and the assembly fastened to the skull with dental acrylic. Stereotaxic coordinates (in mm) were: dorsal cochlear nucleus (DCN) AP = -11.3, ML = ±3.5, DV = -7.0; posterior ventral cochlear nucleus (PVCN): AP = -11.0, ML = ±3.8, DV = -8.2; anterior–ventral cochlear nucleus (AVCN): AP = -9.8, ML = ±4.0, DV = -8.4; inferior colliculus (IC): AP = -8.8, ML = ±1.5, DV = -4.5 (Paxinos and Watson, 1997). Seven animals received one electrode and eight received multiple electrodes. Grass Medical Instrument (Quincy, MA) subdermal needle electrodes were then inserted at the mastoids behind and at the base of each pinnae (mastoid-to-mastoid recordings are hereafter referred to simply as “mastoid,” or M).

The anesthetic and experimental protocol met all requirements regarding the care and use of small animal subjects in accordance with guidelines of the Beijing Laboratory Animal Center, guidelines of the Canadian Council of Animal Care, and the Policies on the Use of Animals and Humans in Neuroscience Research revised and approved by the Society for Neuroscience (2006).

### 2.2. Auditory stimulation

The acoustic stimulus consisted of a 16 kHz tone pip, either 1 ms or 2 ms duration, amplitude modulated by a 0.5 ms linear rise/fall. Stimulus repetition rate was  $11\text{ s}^{-1}$ . Sound was produced by an Intelligent Hearing Systems high frequency tone generator and delivered monaurally via an air tube placed into the left ear canal. Total sound path length was 30 cm resulting in an acoustic transmission delay of 1 ms, assuring that the tone pip arrived at the ear canal exactly at the termination of any possible stimulus electrical artifact (for the 1 ms stimulus only). The digitized stimulus waveform was delivered by a Berkeley Nucleonics Inc. Model 630 arbitrary function generator running at an internal clock rate of 1.25 MHz (i.e., 1250 data points were required to produce a 1 ms stimulus waveform). Peak stimulus intensity was 80 dB.

### 2.3. EEG recording and data acquisition

Electroencephalographic (EEG) activity was conditioned by Grass P511 amplifiers (band pass 30 Hz – 10 kHz, -6 dB down). Implanted electrodes were referenced to a needle electrode in the foot pad. EEG recording quality was monitored on an oscilloscope and each epoch of sampled data was displayed on the computer screen. Each sample epoch was initiated by triggering the arbitrary function generator that delivered the stimulus waveform independent of concurrent acquisition of EEG data sampled at 100 k/s by a Scientific Solutions LabMaster analog-to-digital converter.

Custom data acquisition software developed for our rodent ABR studies implemented effective on-line artifact rejection. All trials containing extreme amplitudes, most often due to cardiac artifact in the mastoid recording, were rejected and the stimulus repeated (see Galbraith et al., 2006; Fig. 1B).

### 2.4. Computer averaging of ABRs

Each averaged evoked response was based on 500 trials that were free of heart or other large amplitude EEG artifacts. For direct recording from implanted electrodes this number of trials was excessive, since CN and IC waveforms were well-defined and highly stable in the individual trials. Indeed, for some mastoid (M) recordings 500 trials were also excessive, since responses were visible in the individual trials. Nevertheless, the recording procedures remained constant to allow for mastoid recordings with reduced signal-to-noise properties. Final averaged ABR waveforms were displayed and saved for later off-line analysis.

### 2.5. Off-line data analysis

ABR peaks were automatically detected by the computer, but with experimenter cursor correction in the event of error. The cursor positions defined the absolute peak latencies (taking into account the 1 ms acoustic delay). The results were plotted using MATLAB (The MathWorks, Natick, MA). Within-animal

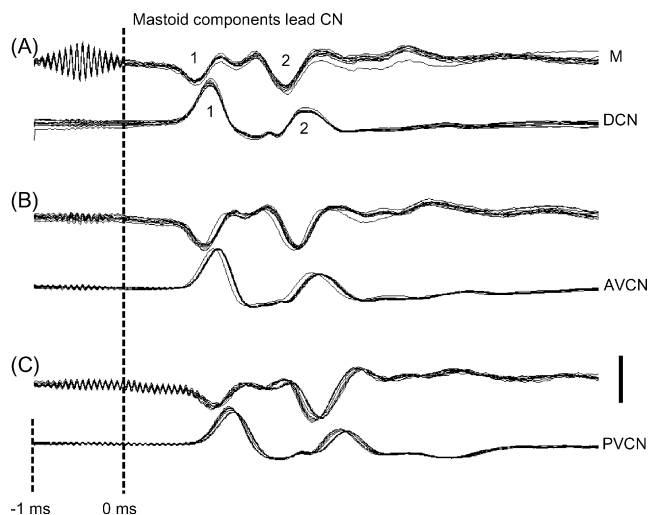


Fig. 1. Pairs of traces comparing short-latency auditory evoked potential components recorded from transversely oriented (mastoid-to-mastoid) subdermal needle electrodes (M) vs. potentials recorded from electrodes acutely implanted in cochlear nucleus (DCN). The results illustrate the consistent finding that components recorded from M immediately precede correlated components recorded from CN. (A) Ten superimposed responses from mastoid (top) and dorsal cochlear nucleus (bottom) evoked by a 1 ms, 16 kHz tone pip. Numbers represent the ordinal position of two initial evoked response components that are highly reliable across conditions and animals. (B) Superimposed responses from anterior–ventral cochlear nucleus (AVCN) in a second animal evoked by a 1 ms tone. (C) Superimposed responses from posterior–ventral cochlear nucleus (PVCN) in a third animal evoked by a 2 ms tone. The short vertical dashed line marks the beginning of the stimulus electrical artifact (–1 ms). The long vertical dashed line defines 0 ms, the exact arrival time of sound at the ear due to acoustic propagation over a 30 cm air tube (and exact duration of the briefer 16 kHz tone pip). Vertical calibration bar equals 5  $\mu$ V (M) and 50  $\mu$ V (CN) for all plots.

comparisons of ABR latencies and conduction times were by *t*-tests for correlated data. In the event that significant differences were not found between different regions of CN the data were treated as independent and grouped in the analyses.

## 2.6. Histology

At the end of testing the animal was euthanized with an overdose of chloral hydrate. Lesion was made at the recording electrode tip by an anodal dc current (500  $\mu$ A for 10 s). The brains were removed, stored in 10% formalin with 30% sucrose until they sank, and then sectioned at 50  $\mu$ m in the frontal plane in a cryostat (–20 °C) and the sections examined to determine exact locations of the recording electrodes.

## 3. Results

### 3.1. Histology

Histological examinations showed in every case that the implanted electrodes were correctly positioned in the targeted CN or IC nuclei.

### 3.2. Qualitative comparison of transverse mastoid-to-mastoid (M) recordings with direct recordings from cochlear nucleus (CN) and inferior colliculus (IC)

Fig. 1 illustrates repeated recordings from three animals comparing M and CN evoked response components. The results show highly correlated waveform patterns consisting of two major deflections, with peak M latencies always preceding corresponding peaks in CN (i.e.,  $M_1 < CN_1$ ,  $M_2 < CN_2$ ). Moreover, the pattern and latencies of the CN responses appear identical in the three CN nuclei tested (DCN, AVCN and PVCN). These waveform patterns are representative of all recordings in all animals. The initial  $M_1$  component seen here is identical to the P1<sub>T</sub> ABR peak reported by Galbraith et al. (2006).

The pattern of absolute latencies and latency differences are consistent whether the stimulus is 1 ms (Fig. 1A and B) or 2 ms (Fig. 1C) in duration (note that stimulus electrical artifacts verify the stimulus duration). Thus, the latency difference between components 1 and 2, which is approximately 1 ms for the 1 ms stimulus (Fig. 1A and B) remains unchanged for the 2 ms stimulus (Fig. 1C). This confirms that the sequence of components cannot represent simple on- and off-responses to the 1 ms stimulus, but must represent instead a generalized on-response to either the 1- and 2-ms stimulus.

Fig. 2 superimposes repeated recordings in two different animals from M and IC (note the expanded time scale compared with Fig. 1). The results in these animals again show two major initial waves in the mastoid recordings (a third wave in Fig. 2B is individualistic and may record later brainstem generators due to variation in placement of the needle electrodes). Early small deflections in the IC recordings are also apparent, but their brief latencies and relatively low amplitudes suggest that they are far-field potentials originating elsewhere, bearing resemblance to the CN potentials seen in Fig. 1.

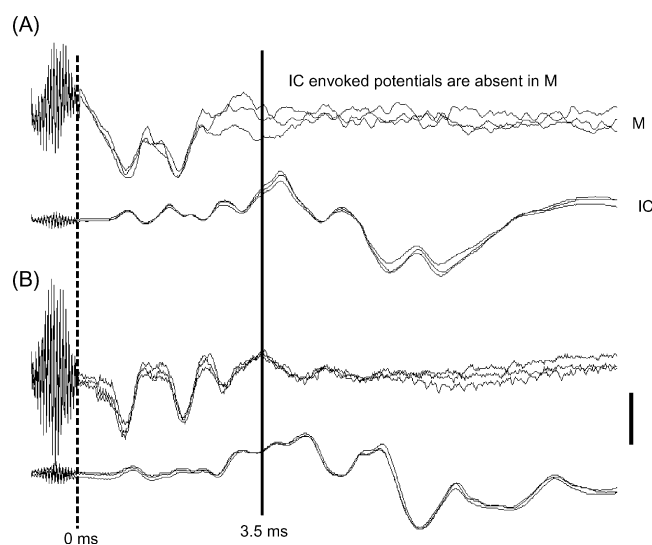


Fig. 2. Data from two animals comparing evoked responses in mastoid-to-mastoid (M) recordings with inferior colliculus (IC); the plot time scale is increased (compared with Fig. 1) to show later IC components. The results show that well-defined, large amplitude, responses in IC are totally absent in M. The solid vertical line is placed 3.5 ms following arrival of sound at the ear.

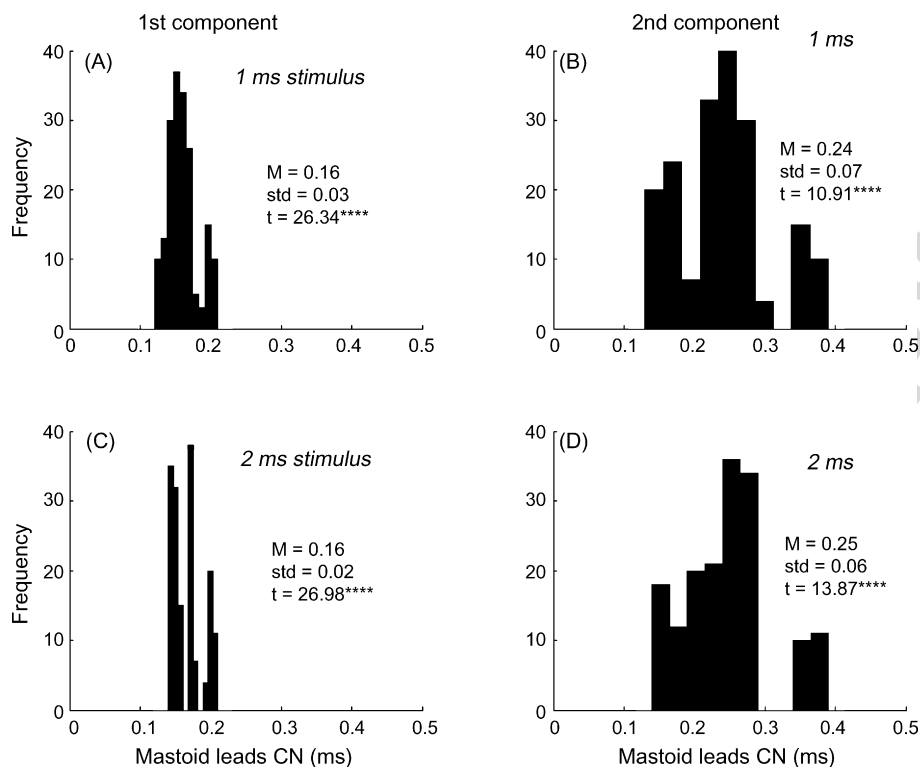


Fig. 3. Frequency histograms of central conduction times (CN – M) with means and standard deviations. The results are based on 350 pairs of waveforms (data from dorsal, anterior–ventral and posterior–ventral CN are combined) computed for the first (CN<sub>1</sub> – M<sub>1</sub>) and second (CN<sub>2</sub> – M<sub>2</sub>) evoked potential components (see Fig. 1). The results show without exception that scalp components always precede cochlear nucleus by more than 0.1 ms. (A and B) First and second components, respectively, evoked by 1 ms tone pip ( $N = 190$ ). (C and D) First and second components, respectively, evoked by 2 ms tone pip ( $N = 160$ ). The  $t$ -values shown in each plot test the null hypothesis that CN – M central conduction times do not differ from zero; results are based on average values computed for each of 15 animals (d.f. = 14, all  $^{****}p$ -values < 0.0001).

What is especially important to note in Fig. 2 is that the large amplitude IC components seen beyond 3.5 ms (vertical solid line) are totally absent in the mastoid recordings. Indeed, beyond 3.5 ms the M recordings are essentially iso-electric, showing only random noise.

### 3.3. Quantitative measures of mastoid and cochlear nucleus recordings

Fig. 1 shows a consistent pattern for three animals in which M evoked potential components always precede CN. Statistical comparisons of the various latency measures between DCN, AVCN and PVCN failed to yield any significant differences. Therefore, data recorded from the different CN nuclei were combined in all subsequent analyses.

Fig. 3 presents a frequency histogram of the results of 350 recordings obtained from scalp and CN in 15 animals. The  $x$ -axis in each plot represents a measure of central conduction time latencies (i.e., CN – M). All plots show a minimum latency difference greater than 0.1 ms. Moreover, the means and standard deviations for a given component are essentially identical regardless of stimulus duration (cf. Fig. 3A versus C, and Fig. 3B versus D). This provides further evidence that stimulus duration did not affect central conduction times. Although central conduction times were not affected, stimulus duration did slightly but significantly affect absolute latencies of the first (M<sub>1</sub>) (mean

[1 ms] = 0.87 ms, mean [2 ms] = 0.90 ms,  $t_{14} = 4.17$ ,  $p < 0.01$ ) and second (M<sub>2</sub>) (mean [1 ms] = 1.87 ms, mean [2 ms] = 1.92 ms,  $t_{14} = 5.33$ ,  $p < 0.01$ ) mastoid components ( $t$ -test for correlated data, computations and degrees of freedom based on average values of the 10 latencies recorded for each animal).

The most striking feature of Fig. 3 is the fact that mastoid components *always* lead contiguous CN components. This consistent pattern of differences in M and CN peak latencies results in highly significant ( $p < 0.0001$ ) differences for the first and second evoked potential component, whether the evoking stimulus is 1 or 2 ms in duration (see  $t$ -values in Fig. 3).

## 4. Discussion

The present study compares short-latency auditory evoked responses recorded from transversely oriented needle electrodes (mastoid-to-mastoid) and electrodes acutely implanted in cochlear nucleus (dorsal, anterior–ventral and posterior–ventral) and inferior colliculus of the rat. Although our results did not show latency differences between the three CN sites tested, the results confirm that unique neural signals are detected by mastoid versus direct brain recordings. Specifically, mastoid components always temporally precede evoked response components in CN (Figs. 1 and 3), but are non-responsive past 3.5 ms which is the latency beyond which well-defined IC components are seen (Fig. 2). These results strongly support the conclusion

that transverse mastoid-to-mastoid recordings reflect an earlier and relatively isolated measure of neural activity that must be distal to the brainstem by more than 0.1 ms (see Fig. 3). The simplest interpretation thus places the mastoid response in the auditory nerve. A similar conclusion has been reached based on less direct evidence in the mouse and rat (Galbraith et al., 2006), as well as for the short-latency brainstem frequency-following response (FFR) in humans (Galbraith, 1994; Galbraith et al., 2000).

The initial component of the mastoid response ( $M_1$ ) must be unambiguously localized to the auditory periphery, since it precedes all responses in the cochlear nucleus, which is the first central synapse in the auditory pathway. Moreover, it also seems likely that the second mastoid component,  $M_2$ , is a peripheral response since it is temporally coupled to  $M_1$ , and precedes the contiguous but delayed  $CN_2$  response. Hence, there is no direct temporal correlate of  $M_2$  in the brainstem. Later M waves (e.g., Fig. 2B), however, may reflect far-field effects emanating from more central auditory nuclei, perhaps the superior olive (not tested here).

While conduction time in the relatively long (2.5 cm) human auditory nerve is about 1 ms (Møller et al., 1988), in smaller animals (rats, guinea pigs and cats) it is on the order of 0.1–0.2 ms (Møller and Jannetta, 1985). These small animal conduction times agree precisely with the 0.16 ms mean values observed in the present study for the first component (Fig. 3A and B).

Mean values and standard deviations of conduction time increased for the second component ( $CN_2 - M_2$ ; Fig. 3B and D), implying a looser temporal coupling. The exact anatomical loci of components farther along the afferent pathway becomes increasingly problematic due to such factors as varied central conduction velocities of auditory neurons, recurrent innervation, fast pathways that bypass some nuclei, etc. (Eggermont, 2001), as well as increasing variability of single unit firing latencies (Huang and Buchwald, 1977). Yet, we argue here that the first and second M and CN components are not actually farther along the auditory pathway, but in fact still are localized to auditory nerve and cochlear nucleus, respectively. The relative increase in conduction time from first to second component must therefore reflect differences in neural processing even within the first central nucleus of the auditory pathway. Comparisons of the stable first component with the more variable second component may thus be useful in future studies of development or the disruption of signal processing due to neuropathology.

The absolute average latency of the initial  $M_1$  component in the present study was 0.87 ms (1 ms stimulus). Using the identical stimulus delivery system and stimulus Galbraith et al. (2006) reported latencies of 0.75 ms or longer. Such latencies exceed those reported by Møller and Jannetta (1985) in small animals. However, the values reported by Møller and Jannetta resulted from a brief (0.1 ms) acoustic click, whereas in the present study the stimulus consisted of tone pips with 0.5 ms rise time. Thus, additional time would be required following tone onset before an effective neural threshold level could be reached, thereby introducing additional delay.

The surgical procedures required to secure the implanted electrodes to the exposed skull made it impossible to record

from scalp needle electrodes oriented in a midline plane orthogonal to the mastoid electrodes. Yet, when this is done (Galbraith et al., 2006) such midline responses bear a striking similarity to the CN responses seen in the present study. These similarities include midline response latencies that always lag behind mastoid, and first component conduction times between mastoid and midline that are nearly identical to those reported here (0.16 ms in the present study versus 0.10 ms in Galbraith et al.). This strongly supports the conclusion that early midline recordings via scalp needle electrodes reflect neural responses in the cochlear nucleus, while transverse mastoid electrodes effectively isolate an earlier peripheral response. Of course, all later components recorded using needle electrodes must necessarily reflect activity originating farther along the auditory pathway.

In conclusion, the present results confirm that it is possible to effectively isolate specific short-latency auditory evoked response components, especially the earliest waves attributed to auditory nerve. This is accomplished by the simple technique of using subdermal needle electrodes to record a transverse dipole from mastoid-to-mastoid. Standard single channel recordings (e.g., Bok et al., 2003) confound these potentials and do not yield clearly separable components that differ by as little as one-tenth of a millisecond. Thus, the origin of short-latency mastoid responses is clarified, making it possible to obtain more precise and selective measurements of neural signals in early stages of the afferent auditory pathway. The technique reported here thus allows for precise and repeated non-invasive measurements of central conduction time in mouse and rat strains that have suspected or induced hearing loss, or neuro-developmental defects of the central nervous system (CNS). Moreover, because similar response patterns are observed in the mastoid-to-mastoid responses of humans (Galbraith, 1994; Galbraith et al., 2000), it is possible that our recording technique will provide useful and novel information in the clinical assessment of auditory prosthesis devices, such as the assessment of new signal-processing strategies used in cochlear implants (Chen et al., in press).

## Acknowledgments

This work was supported by the China Natural Science Foundation (No. 60535030), a “985” Grant from Peking University, and United States NIH Grant HD 04612.

## References

- Bok D, Galbraith G, Lopez I, Woodruff M, Nusinowitz S, et al. Blindness and auditory impairment caused by loss of the sodium bicarbonate cotransporter NBC3. *Nat Genet* 2003;34:313–9.
- Chen J, Wu X-H, Li L, Chi H-S. Simulated phase-locking stimulation: an improved speech processing strategy for cochlear implant. *J Otorhinolaryngol*, in press.
- Eggermont J. Between sound and perception: reviewing the search for a neural code. *Hear Res* 2001;157:1–42.
- Galbraith GC. Two-channel brainstem frequency-following responses to pure tone and missing fundamental stimuli. *Electroencephalogr Clin Neurophysiol* 1994;92:321–30.
- Galbraith GC, Threadgill MR, Hemsley J, Salour K, Songdej N, Ton J, et al. Putative measure of peripheral and brainstem frequency-following in humans. *Neurosci Lett* 2000;292:123–7.

- Galbraith G, Waschek J, Armstrong B, Edmond J, Lopez I, Liu W, et al. Murine auditory brainstem evoked response: putative two-channel differentiation of peripheral and central neural pathways. *J Neurosci Methods* 2006;153:214–20.
- Henry KR. Auditory brainstem volume-conducted responses: origins in the laboratory mouse. *J Am Audiol Soc* 1979;4:173–8.
- Huang CM, Buchwald JS. Interpretation of the vertex short-latency acoustic response: a study of single neurons in the brain stem. *Brain Res* 1977;137:291–303.
- Møller AR, Jannetta PJ. Neural generators of the auditory brainstem response. In: Jacobson JT, editor. *The auditory brainstem response*. San Diego, CA: College-Hill Press; 1985. p. 13–31.
- Møller AR, Jannetta PJ, Sekhar LN. Contributions from the auditory nerve to the brainstem auditory evoked potentials (BAEPs): results of intracranial recordings in man. *Electroencephalogr Clin Neurophysiol* 1988;71:198–211.
- Parham K, Sun X-M, Kim DO. Noninvasive assessment of auditory function in mice: auditory brainstem response and distortion product otoacoustic emissions. In: Willott JF, editor. *Handbook of mouse auditory research: from behavior to molecular biology*. Boca Raton, FL: CRC Press; 2001. p. 37–58.
- Paxinos G, Franklin KBJ. *The mouse brain in stereotaxic coordinates*. 2nd ed. New York, NY: Academic Press; 2001.

Author's personal copy